NeuroImage 65 (2013) 280–287

Contents lists available at SciVerse ScienceDirect

NeuroImage

journal homepage: www.elsevier.com/locate/ynimg

Cranial electrotherapy stimulation and transcranial pulsed current stimulation: A computer based high-resolution modeling study

Abhishek Datta [a,b,*], Jacek P. Dmochowski [a], Berkan Guleyupoglu [a], Marom Bikson [a], Felipe Fregni [b,c,**]

[a] Neural Engineering Laboratory, Department of Biomedical Engineering, The City College of New York of CUNY, New York, NY 10031, USA
[b] Laboratory of Neuromodulation, Spaulding Rehabilitation Hospital, Harvard Medical School, Boston, MA 02114, USA
[c] Berenson-Allen Center for Noninvasive Brain Stimulation, Beth Israel Deaconess Medical Center, Harvard Medical School, Boston, MA 02215, USA

ARTICLE INFO

Article history:
Accepted 24 September 2012
Available online 5 October 2012

Keywords:
Cranial electrotherapy stimulation
CES
Brain stimulation
Computer based modeling
Brainstem

ABSTRACT

The field of non-invasive brain stimulation has developed significantly over the last two decades. Though two techniques of noninvasive brain stimulation — transcranial direct current stimulation (tDCS) and transcranial magnetic stimulation (TMS) — are becoming established tools for research in neuroscience and for some clinical applications, related techniques that also show some promising clinical results have not been developed at the same pace. One of these related techniques is cranial electrotherapy stimulation (CES), a class of transcranial pulsed current stimulation (tPCS). In order to understand further the mechanisms of CES, we aimed to model CES using a magnetic resonance imaging (MRI)-derived finite element head model including cortical and also subcortical structures. Cortical electric field (current density) peak intensities and distributions were analyzed. We evaluated different electrode configurations of CES including in-ear and over-ear montages. Our results confirm that significant amounts of current pass the skull and reach cortical and subcortical structures. In addition, depending on the montage, induced currents at subcortical areas, such as midbrain, pons, thalamus and hypothalamus are of similar magnitude than that of cortical areas. Incremental variations of electrode position on the head surface also influence which cortical regions are modulated. The high-resolution modeling predictions suggest that details of electrode montage influence current flow through superficial and deep structures. Finally we present laptop based methods for tPCS dose design using dominant frequency and spherical models. These modeling predictions and tools are the first step to advance rational and optimized use of tPCS and CES.

© 2012 Elsevier Inc. All rights reserved.

Introduction

The field of non-invasive brain stimulation has developed significantly during the last two decades. The use of neurophysiological, neuroimaging and computer-based modeling tools have contributed to this increased interest and development of this field. As a consequence, techniques that have been explored and used in the past are now being re-explored, with different, optimized parameters of stimulation. Transcranial direct current stimulation is one such example. The use of neurophysiological markers such as transcranial magnetic stimulation-induced cortical excitability and computer-based modeling has optimized parameters of stimulation such as electrode montage, intensity and duration of stimulation (Brunoni and Fregni, 2011; Datta et al., 2008, 2010; Miranda et al., 2006; Nitsche and Paulus, 2000; Wagner et al., 2006, 2007) One highly used method of noninvasive transcranial electrical stimulation — cranial electrotherapy stimulation (CES), with relatively broad clinical use, has not been fully explored.

CES has had relatively broad clinical use following FDA clearance in 1978, and is historically a derivative of neuromodulation approaches dating to the early 20th century including cranial electrostimulation therapy (CET) and electrosleep (ES). CES devices use transcranial pulse current stimulation with dose parameters typically 50 μA to 5 mA intensity, around 100 Hz, typically applied over a session (around 30 min) using surface electrodes on the infra- or supra-auricular structures (Zaghi et al., 2010). Although the CES technique has been used for several decades (Edelmuth et al., 2010) and has been reported to be effective for the treatment of insomnia, depression and anxiety (FDA label indications) in several clinical studies, the mechanisms of action remain unknown. Due to its effect mainly on vegetative symptoms of psychiatric disorders such as sleep, impaired attention and fatigue, it is purported that the application of CES through the maxillo-occipital junction causes current to reach the sub-cortical and brain stem structures. It has been shown that stimulation of these structures causes increased secretion of neurotransmitters, namely serotonin,

* Correspondence to: A. Datta, T-463 Steinman Hall, Grove School of Engineering, The City College of CUNY, 160 Convent Ave, New York, NY 10031, USA. Fax: +1 212 6506727.
** Correspondence to: F. Fregni, Spaulding Rehabilitation Hospital, 125 Nashua Street, Boston, MA 02114, USA. Fax: +1 617 975 5322.
E-mail addresses: abhishek.datta@gmail.com (A. Datta), ffregni@partners.org (F. Fregni).

1053-8119/$ – see front matter © 2012 Elsevier Inc. All rights reserved.
http://dx.doi.org/10.1016/j.neuroimage.2012.09.062

beta endorphin, and norepinephrine (Shealy, 1989); thus being potentially involved with the mechanisms underlying the behavioral effects of CES (Schroeder and Barr, 2001).

In one of the few controlled studies where the physiologic mechanism of action of CES was investigated, electroencephalographic (EEG) changes were reported (Schroeder and Barr, 2001). CES led to changes in alpha and beta frequency ranges suggesting potential neuroplastic and cognitive effects of this technique. Interestingly, similar changes in alpha and beta bands were shown to be associated with a reduction in the emotional-cognitive aspects of pain in a study using transcranial direct current stimulation, which is another type of non-invasive brain stimulation (Maeoka et al., 2012). Though these results are promising, additional studies must be done due to the lack of mechanistic studies, particularly in CES (Edelmuth et al., 2010). Table 1 includes a summary of the most recent studies with CES therapy published in the past 15 years. Moreover a recurring point of contention over the years has been whether low current CES applied through the electrode sites (ear lobes, mastoid processes or the temporal areas) can even reach the underlying cortex to influence neural activity. In fact very limited effort has been invested to quantify the spatial distribution of currents within the human brain using this technique.

Since it is technically difficult to directly assess current flow in structures within the human head, simulations of current flow via computer modeling can be used to predict the intensity and spatial distribution of current flow during transcranial stimulation. Concentric-sphere models have previously been used to calculate CES induced electric fields (Ferdjallah et al., 1996). In recent years, advances in modeling and imaging tools have allowed the development of models with increased realism and precision, resulting in high-resolution (1 mm^3) MRI derived head models that capture gyri/sulci anatomical details (Datta et al., 2009) as well as examine current density distributions through sub-cortical target regions (Dasilva et al., 2012; Parazzini et al., 2012).

We adapted a previously developed high-resolution individualized model of tDCS (Datta et al., 2009) for simulating the effects of CES. We modeled the conventional ear-clip electrode montage and compared it with several novel montages (Brain Gear, Switzerland). We determined induced surface cortical electrical field (EF) to predict spatial focality. In addition, sub-cortical and brain-stem structures implicated in the purported CES beneficial effects were individually analyzed.

Methods

In order to better understand which brain regions are modulated during cranial electrotherapy stimulation (CES), we carried out a high-resolution finite element (FE) model analysis. For comparison, we showed the effects of conventional therapy using ear-clip electrodes versus multiple novel montages like the in-ear, ear-hook and the over-the-ear montages.

MRI derived high-resolution model

The human head model was derived from a high spatial resolution (1 mm^3) 3 T MRI of a male adult healthy subject with no neurological pathologies. Using a combination of tools from FMRIB Software Library (FSL) and Simpleware, the head model was segmented into tissue compartments representing the scalp, skull, CSF, eye region, muscle, gray matter, white matter, and air respectively. In addition to analyzing current flow patterns through structures thought to be implicated in the beneficial effects of CES, structures such as cingulate cortex, thalamus, insula, pituitary gland, pineal gland, hypothalamus, midbrain, pons, and medulla oblongata were also segmented. The head model was limited to the masks being directly derived from the MRI acquisition volume. An artificial neck and shoulder region was thus fused onto the existing segmented head. Stimulation electrodes of various sizes (as mentioned below) were imported as CAD models and placed onto the existing segmented volume to model the different CES montages. The entire model (head and the electrodes) were meshed and exported to a commercial FE solver (COMSOL 3.5a) for final computation of current flow patterns.

Electrode montages

We modeled the following CES montages representing the conventional and the novel montages (see Fig. 1):

1) Conventional ear-clip montage (montage 1):The stimulation electrodes were placed mimicking conventional CES stimulation using ear-clip electrodes. The left ear-clip electrode was energized to a normal current density boundary condition corresponding to 1 mA total injected current. The right ear-clip electrode was applied as the ground boundary condition. All other external surfaces were treated as insulated.
2) Novel in-ear electrode montage (montages 2 and 3):Stimulation electrodes were placed resembling the in-ear headphone locations. The left in-ear electrode was energized to a normal current density boundary condition corresponding to 1 mA total injected current. The right in-ear electrode was applied as the ground boundary condition. All other external surfaces were treated as insulated. In addition, the In-Ear electrode montage was also solved at 150 Hz (montage 3).
3) Novel ear-hook electrode montage (montage 4):Stimulation electrodes were placed resembling the ear-hook headphone locations. The left ear-hook electrode was energized to a normal current density boundary condition corresponding to 1 mA total injected current. The right ear-hook electrode was applied as the ground boundary condition. All other external surfaces were treated as insulated.
4) Novel over-the-ear electrode montage (4 contacts) (montage 5): Stimulation electrodes were placed resembling the over-the-ear

Table 1
Summary of randomized CES trials.

Author	Year	Patient#	Design	Sham controlled	Blinded	Clinical effects
Rose	2009	44	Parallel Randomized Trial	Yes	Double blinded	The CES group showed improvements in sleep disturbance, and depression though neither was statistically significant.
Schroeder	2001	12	Cross-over Trial	Yes	Double blinded	.5 and 100 Hz CES elicited frequency distribution shifts. 100 Hz CES produced greater overall change. These results suggest beneficial changes in mental state.
Southworth	1999	52	Parallel Randomized Trial	Yes	Not Stated	CES significantly improved attention and concentration in a normal adult population.
Scherder et al.,	2006	21	Parallel Randomized Trial	Yes	Blinded	No significant improvements on cognition and (affective) behavior were found between CES treatment and control groups.

Abbreviations: CES: cranial electrical stimulation; TCES: transcutaneous cranial electrical stimulation; CBF: cerebral blood flow.

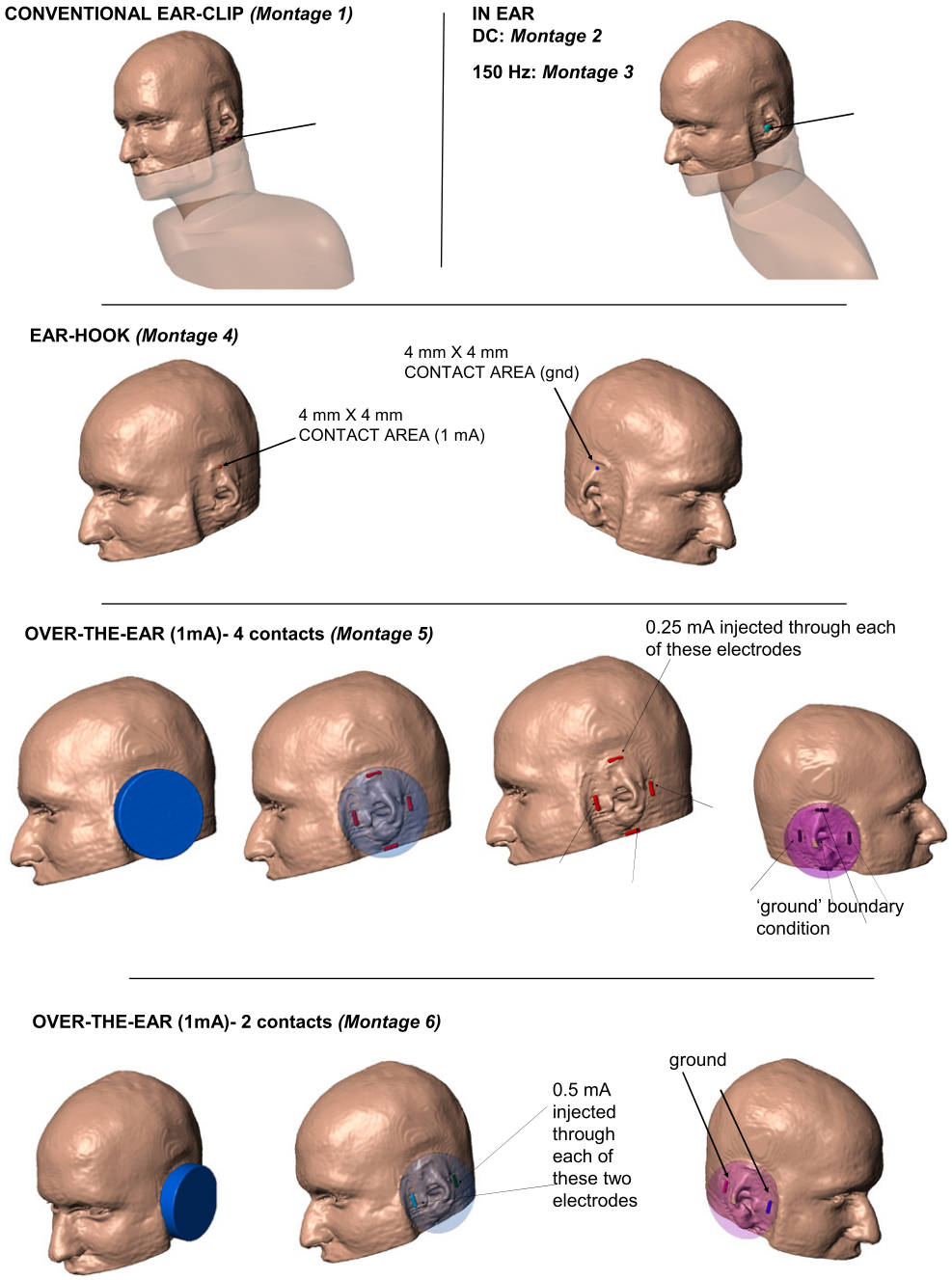

Fig. 1. Cranial electrotherapy stimulation (CES)/transcranial pulsed current stimulation (tPCS) electrode montages modeling in the present study.

headphone locations. The four left over-the-ear electrodes were each energized to a normal current density boundary condition corresponding to 0.25 mA current (leading to 1 mA total current injected across the head). The four right over-the-ear electrodes were each applied as the ground boundary condition. All other external surfaces were treated as insulated.

5) Novel over-the-ear electrode montage (2 contacts) (montage 6): Stimulation electrodes were placed resembling the over-the-ear headphone locations. The two left over-the-ear electrodes were each energized to a normal current density boundary condition corresponding to 0.5 mA current (leading to 1 mA total current injected across the head). The two right over-the-ear electrodes were each applied as the ground boundary condition. All other external surfaces were treated as insulated.

The Laplace equation was solved and induced cortical surface electric field (EF) magnitude maps for the different electrode montages were determined. The following isotropic electrical conductivities at DC in (S/m) were assigned: scalp (0.465); skull (0.01); CSF (1.65); gray matter (0.276); white matter (0.126); eye (0.4); muscle (0.334); hypothalamus (0.201); glands (0.5); air (1e−15); and electrode (5.8e7). The following isotropic electrical conductivities corresponding to 150 Hz in (S/m) were assigned: scalp (0.002); skull (0.02); CSF (1.65); gray matter (0.092); white matter (0.059); eye (0.4); muscle (0.282); hypothalamus (0.075); glands (0.522); air (1e−15); and electrode (5.8e7). The cingulate cortex, insula, and the thalamus were assigned gray matter conductivity while the midbrain, pons, and the medulla oblongata were assigned white matter conductivity (DaSilva et al., 2012; Gabriel et al., 1996).

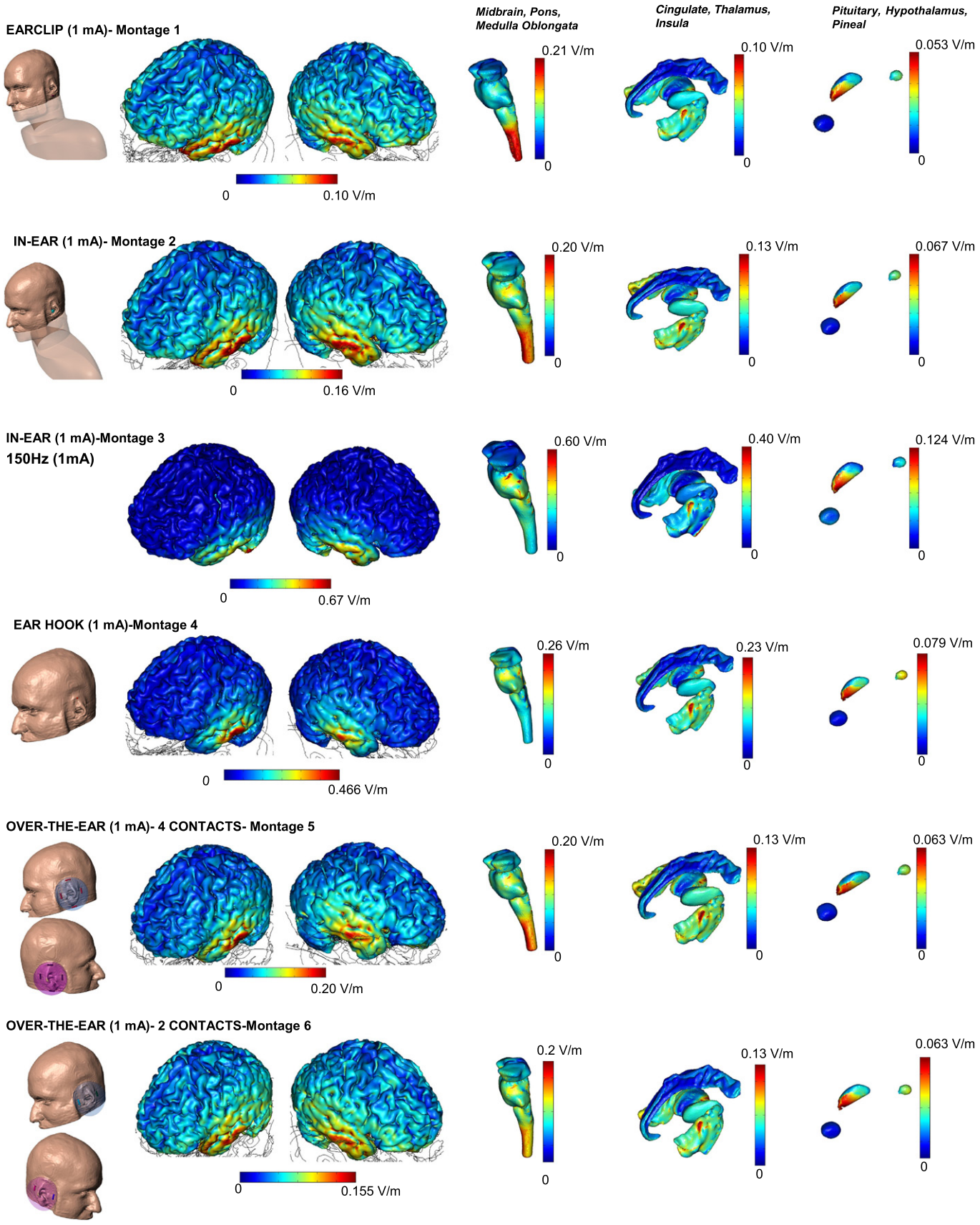

Fig. 2. Cortical surface electric field magnitude plots for cortical, subcortical and brain-stem regions across all montages. All plots are plotted to their maximum peak.

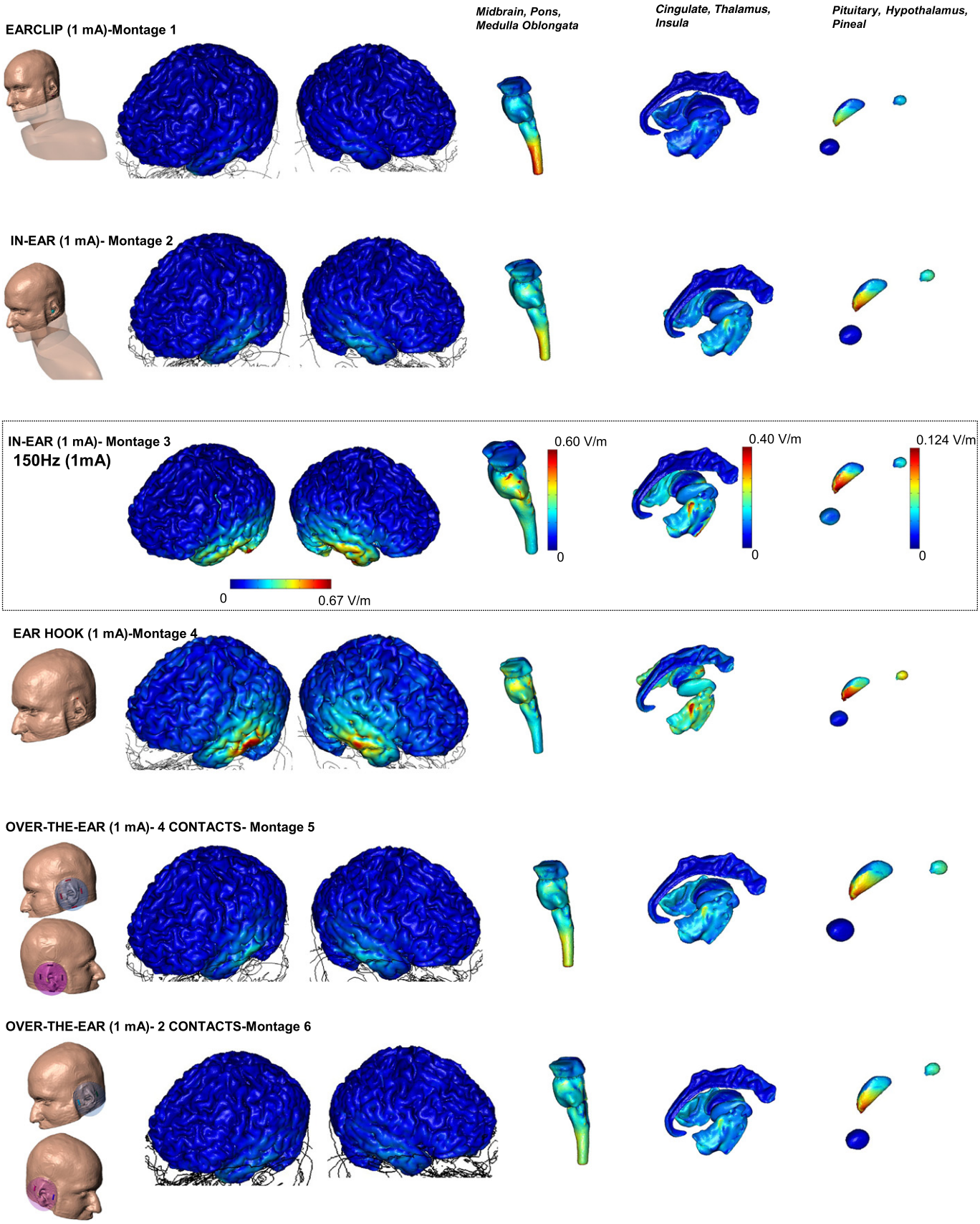

Fig. 3. Cortical surface electric field magnitude plots for cortical, subcortical and brain-stem regions across all montages. The ear-hook montage led to the maximum peak induced electric field magnitude and all plots are scaled to this maximum peak (apart from montage 3 — 150 Hz simulation).

Table 2
Different classes of tPCS are summarized including temporal waveform (function), the associated magnitude spectrum (frequency content), and clinical references including dose using "CES". The Fourier series were generated using the same parameters for T, τ, and A across all classes and the same parameters for h, D0, Ton, and Toff where applicable. Note that n is a discrete function of 1/T (or Toff in the case of Class III). In Class III, the CES case would have D0 set to zero which would lower the peak at zero. In Class II, hr = (h + 1)/h, in Class III, Tr = Ton/Toff and in all classes, P = A(τ/T). The references indicated are: [1]Limoge et al. (1999), [2]Brown (1975), [3]Bystritsky et al. (2008), [4]http://www.net1device.com/specs.htm, [5]Liss Stimulator Manual, Model No. SBL-502-B, [6]Richthofen and Mellor (1979), [7]Dimitrov and Ralev (2009), [8]Liss Stimulator Manual, Model No.SBL-501-M.

	Waveform	Magnitude spectrum	Notes
Class I(A) - Monophasic pulse	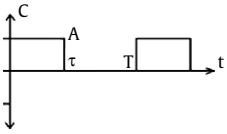	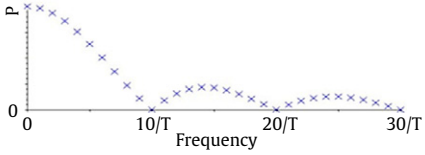	-ES[2] -CET[6] -EA[2]
Class I(B) - Monophasic pulse with DC offset	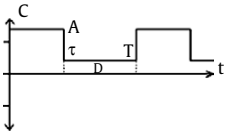	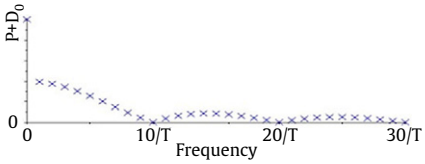	-ES[2,6] -EA[2] -CET[2,6] -TCET[6,2]
Class II(A) - Biphasic pulse	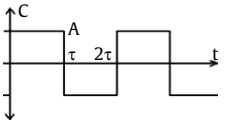	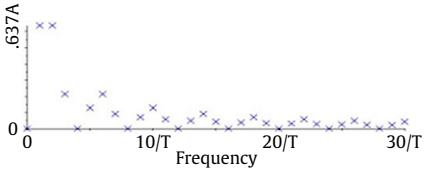	-CES[7]
Class II(B) - Biphasic pulse with delay	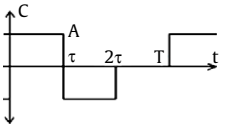	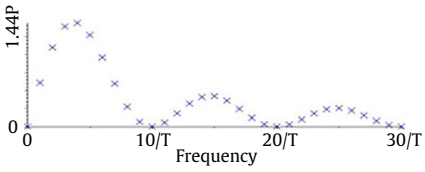	-TCET -CET -NET[4] -CES[5]
Class II(C) - Asymmetric biphasic pulse	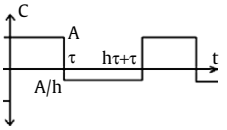	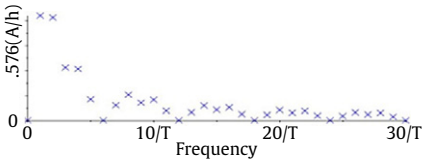	
Class II(D) - Asymmetric biphasic pulse with delay	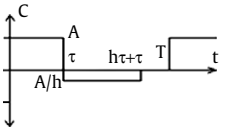	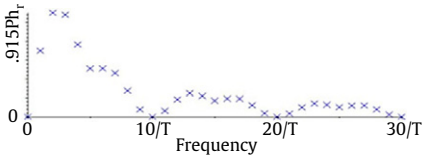	-CES[3] -NET
Class III - Monophasic pulse train	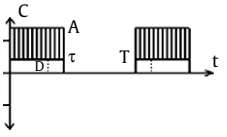	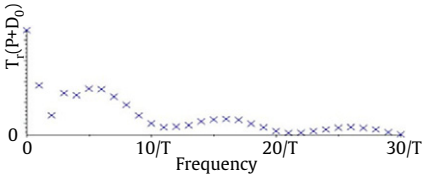	-LC[1] -TCES[1] -CES[8]

Results

Figs. 2 and 3 summarize results using each electrode montage. In Fig. 2, all panels are scaled to their individual peak electric field magnitude (peak/scale indicated), which highlights the electric field local maximum in each case and the regional spatial distribution. In Fig. 3, each cortical and sub-cortical column is re-scaled to one value (peak of the ear-hook montage) to highlight the *relative* electric field intensities and distributions across montages (except for the 150 Hz case).

The conventional ear-clip montage resulted in a 0.10 V/m peak induced cortical electric field. Maximal currents were induced in the temporal sides of the cortex and in the medulla oblongata (see Discussion) with diffuse activation in the midbrain, pons, thalamus, insula, and hypothalamus.

For the in-ear montage, a similar spatial profile of induced currents was predicted; however the peak induced electric field in the cortex was higher (0.16 V/m). The in-ear montage thus led to higher induced EF magnitudes in the midbrain, pons, hypothalamus, and the insula.

The ear-hook montage led to the highest peak induced cortical electric fields for any montage tested in this series (0.47 V/m) as well as higher electric field in several deeper brain structures, with a notable exception of the medulla oblongata presumably reflecting more superior current flow through the middle of the brain.

The over-the-ear montage using either 2 or 4 contacts led to similar current activation (peak and spatial profile) in the sub-cortical and the brain stem regions. The 2 contact montage however led to a marginally reduced peak induced electric field in the cortex in comparison to the 4 contact montage.

Only for the in-ear montage, we further considered the 150 Hz simulation model. Though the peak electric field increased, it did so relatively uniformly (i.e. the relative spatial pattern of current flow was qualitatively unchanged; see discussion).

Discussion

The objectives of this study were to (i) determine the magnitude of current that reaches brain regions implicated in CES behavioral actions and (ii) compare across conventional ear-clip montage with novel montages to assess the sensitivity of brain current flow to dose.

Several findings are novel and noteworthy. Firstly, our high-resolution models predict that current passes through the skull and reaches cortical and subcortical areas leading to electric fields of ~0.2–0.6 V/m depending on the model. The prediction that CES-induced current intensities in deep brain structures are not significantly decreased from cortical values, including in the sub-cortical and brainstem regions as well as thalamic nuclei, is potentially clinically meaningful. While deep brain structures stimulation is dependent on electrode montage, in all cases, the predicted peak electric fields generated in at least one sub-cortical region were comparable to that of cortical areas. In some cases, the local maximum in the mid-brain in fact exceed cortical values — a result that can be explained by both current funneling via the foramen magnum and higher white matter tissue resistivity. Most of the CES studies report effects on vegetative symptoms such as sleep, appetite, fatigue, attention and anxiety (Rose et al., 2008, 2009; Southworth, 1999). Given the involvement of subcortical structures located in the brainstem, thalamus and hypothalamus, our findings are consistent with theories implicating these regions in CES effects on these symptoms. These findings are also in agreement with a recent study assessing the effects of CES using Limoge's current on cerebral blood flow (CBF). Interestingly, in this study authors showed no global CBF changes; however they observed significant CBF changes in the brainstem and thalamus (Gense de Beaufort et al., 2012).

The peak electric field magnitudes generated during CES (<1 V/m) are approximately 100–1000 fold lower than electric fields induced by transcranial magnetic stimulation (TMS) or electroconvulsive therapy (ECT) (Bijsterbosch et al., 2012; De Geeter et al., 2012; Deng et al., in press; Lee et al., 2011). This finding is expected as these later approaches (TMS and ECT) lead to supra-threshold neuronal firing. Indeed, animal studies suggest the threshold for activation of quiescent neurons to be ~100 V/m (Jefferys et al., 2003; Radman et al., 2009) and it therefore can be assumed that CES produces sub-threshold field intensities. The electric field magnitude induced by CES is broadly comparable to those induced by tDCS (Datta et al., 2009; Miranda et al., 2006) but the CES waveform is pulsed in contrast to the static (DC) waveform of tDCS. Any cognitive and behavioral changes produced centrally by CES would thus have to result from neurophysiological changes produced by pulsed electric fields up to 0.6 V/m.

While the cellular effects of low-intensity (few V/m) weak DC current on neurophysiology have been characterized using animal models (Bikson et al., 2004; Fritsch et al., 2010; Kabakov et al., 2012) fewer studies have explored stimulation with alternating (AC) or weak pulsed sub-threshold currents. Because weak "sub-threshold" fields are not sufficient in themselves to trigger action potentials, attention has focused on modulation of ongoing activity, especially ongoing oscillations. Weak AC fields down to 0.25 V/m peak (Deans et al., 2007) and 0.2 V/m peak (Reato et al., 2010) can entrain gamma oscillations in brain slices. Pulsed stimulation, with intensities as low as 0.3 V/m, can entrain epileptiform activity in brain slices (Francis et al., 2003). These animal studies at least suggest the feasibility on low-intensity (<1 V/m) alternating/pulsed electric fields interacting with ongoing active neuronal activity. Indeed, many of the structures associated with CES modulation and modeled in this study exhibit ongoing oscillations that are moreover state dependent (Buzsaki et al., 2012).

In addition to the currents being delivered via ear electrodes in CES the use of small AC currents over the scalp has been tested in several studies. This method is called transcranial alternating current stimulation (tACS). In humans, most research on tACS has been shown to enhance visual and somatosensory perception as well as motor learning and control. More recently, studies have begun to investigate the effects of tACS on higher cognitive functions and changes such as decision-making and risk taking functions have been shown (Feurra et al., 2012; Paulus, 2012). Besides important similarities between tACS and CES, different locations of electrode montages and parameters of stimulation make CES underlying mechanisms including current fields unique as shown in this article. We believe therefore that it is important that CES is labeled differently. Given the modern labeling of techniques of non-invasive brain stimulation, CES can be referred as tPCS (transcranial pulsed current stimulation).

Our models provide insight into the role of electrode montage in CES optimization. Even relatively minor changes in CES electrode montage altered peak brain electric field and overall brain current flow patterns. For example, the ear-hook montage produced the highest relative cortical and sub-cortical electric field, though with higher spatial focality. Though further clinical research is required to isolate which regions should be targeted based on symptomology, computational forward models provide a tool for studying clinical indications and even subject specific optimization. Indeed, much of the sophistication developed for tDCS modeling may be leveraged for CES (Dmochowski et al., 2011; Halko et al., 2011). Here we considered current flow in a single subject and did not study potential inter-individual differences such as differences in anatomy (Datta et al., 2012).

Our observation of stimulation clustering during CES reinforces the importance of models incorporating correct sulci/gyri resolution as in tDCS modeling (Datta et al., 2009; Datta et al., 2011). Similarly, as shown, detailed current flow patterns in sub-cortical structures require precise segmentation of these regions. It is also important to further optimize model methodology for CES montages and waveforms. We compared static (DC) and 150 Hz conductivity for one montage and observed significant changes in peak electric field, though little difference was seen in relative current distribution — this provides an initial indication of the range of electric fields expected (0.2 to 1 V/m) and support the generally applied comparisons across montages. None-the-less, detailed study (Bikson and Datta, 2012) of tissue type, tissue inhomogeneity and anisotropy (Lee et al., 2012; Suh et al., 2010) will increase model accuracy. Development of appropriate computational models of CES may enhance technologic development and dose optimization, potentially enhancing the efficacy and rigor of CES clinical trials.

Finally, we note that CES is in fact a derivative of clinical neuromodulation approaches evaluated over decades including electrosleep (ES), transcerebral electrotherapy (TCET), and cranial electrostimulation therapy (CET), and developed alongside approaches such as electroanesthesia (EA), transcutaneous cranial electrical stimulation (TCES), neuroelectric therapy (NET) and Limoge current (LC). These approaches are forms of transcranial pulsed current stimulation and each characteristic waveform produces a unique frequency content (Table 2) from which a dominant frequency can be identified. We adapted CCNY-SPHERES (www.neuralengr.com/spheres), a laptop based forward model program based on concentric spheres, for tPCS. While this approach considers each frequency independently and

concentric spheres evidently do not represent cortical folding or explicit deep brain structures, CCNY-SPHERES provides an immediately accessible tool for dose exploration using tPCS. High-resolution FEM models, as developed in this study, are more resource intensive, and may thus be evaluated on those dose approaches considered promising based on CCNY-SPHERES pre-screening.

Acknowledgments

This work was partially funded by a gift from *To Be First AG* to the Laboratory of Neuromodulation, Spaulding Rehabilitation Hospital (M.B and A.D.). We are thankful to Noelle Chiavetta for her editorial revision on this manuscript.

References

Bijsterbosch, J.D., Barker, A.T., et al., 2012. Where does transcranial magnetic stimulation (TMS) stimulate? Modelling of induced field maps for some common cortical and cerebellar targets. Med. Biol. Eng. Comput. 50 (7), 671–681.
Bikson, M., Datta, A., 2012. Guidelines for precise and accurate computational models of tDCS. Brain Stimul. 5 (3), 430–431.
Bikson, M., Inoue, M., et al., 2004. Effects of uniform extracellular DC electric fields on excitability in rat hippocampal slices in vitro. J. Physiol. 557 (Pt. 1), 175–190.
Brunoni, A.R., Fregni, F., 2011. Clinical trial design in non-invasive brain stimulation psychiatric research. Int. J. Methods Psychiatr. Res. 20 (2), e19–e30.
Buzsaki, G., Anastassiou, C.A., et al., 2012. The origin of extracellular fields and currents — EEG, ECoG, LFP and spikes. Nat. Rev. Neurosci. 13 (6), 407–420.
Dasilva, A.F., Mendonca, M.E., et al., 2012. tDCS-induced analgesia and electrical fields in pain-related neural networks in chronic migraine. Headache.
Datta, A., Bansal, V., et al., 2009. Gyri-precise head model of transcranial direct current stimulation: improved spatial focality using a ring electrode versus conventional rectangular pad. Brain Stimul. 2 (4), 201–207 (207 e201).
Datta, A., Bikson, M., et al., 2010. Transcranial direct current stimulation in patients with skull defects and skull plates: high-resolution computational FEM study of factors altering cortical current flow. Neuroimage 52 (4), 1268–1278.
Datta, A., Elwassif, M., et al., 2008. Transcranial current stimulation focality using disc and ring electrode configurations: FEM analysis. J. Neural Eng. 5 (2), 163–174.
Datta, A., Baker, J.M., et al., 2011. Individualized model predicts brain current flow during transcranial direct-current stimulation treatment in responsive stroke patient. Brain Stimul. 4 (3), 169–174.
Datta, A., Truong, D., et al., 2012. Inter-individual variation during transcranial direct current stimulation and normalization of dose using MRI-derived computational models. Front. Psychiatry 3 (91). http://dx.doi.org/10.3389/fpsyt.2012.0009191.
De Geeter, N., Crevecoeur, G., et al., 2012. A DTI-based model for TMS using the independent impedance method with frequency-dependent tissue parameters. Phys. Med. Biol. 57 (8), 2169–2188.
Deans, J.K., Powell, A.D., et al., 2007. Sensitivity of coherent oscillations in rat hippocampus to AC electric fields. J. Physiol. 583 (Pt. 2), 555–565.
Deng, Z.D., Lisanby, S.H., et al., in press. Electric field depth-focality tradeoff in transcranial magnetic stimulation: simulation comparison of 50 coil designs. Brain Stimul. http://dx.doi.org/10.1016/j.brs.2012.02.005.
Edelmuth, R.C., Nitsche, M.A., et al., 2010. Why do some promising brain-stimulation devices fail the next steps of clinical development? Expert Rev. Med. Devices 7 (1), 67–97.
Ferdjallah, M., Bostick Jr., F.X., et al., 1996. Potential and current density distributions of cranial electrotherapy stimulation (CES) in a four-concentric-spheres model. IEEE Trans. Biomed. Eng. 43 (9), 939–943.
Feurra, M., Galli, G., et al., 2012. Transcranial alternating current stimulation affects decision making. Front. Syst. Neurosci. 6 (39), 1–2.
Francis, J.T., Gluckman, B.J., et al., 2003. Sensitivity of neurons to weak electric fields. J. Neurosci. 23 (19), 7255–7261.
Fritsch, B., Reis, J., et al., 2010. Direct current stimulation promotes BDNF-dependent synaptic plasticity: potential implications for motor learning. Neuron 66 (2), 198–204.
Gabriel, C., Gabriel, S., Corthout, E., 1996. The dielectric properties of biological tissues: I. Literature survey. Phys. Med. Biol. 41 (11), 2231–2249 (Nov, Review).
Gense de Beaufort, D., Sesay, M., et al., 2012. Cerebral blood flow modulation by transcutaneous cranial electrical stimulation with Limoge's current. J. Neuroradiol. 39 (3), 167–175.
Halko, M.A., Datta, A., et al., 2011. Neuroplastic changes following rehabilitative training correlate with regional electrical field induced with tDCS. Neuroimage 57 (3), 885–891.
Jefferys, J.G., Deans, J., et al., 2003. Effects of weak electric fields on the activity of neurons and neuronal networks. Radiat. Prot. Dosimetry 106 (4), 321–323.
Kabakov, A.Y., Muller, P.A., et al., 2012. Contribution of axonal orientation to pathway-dependent modulation of excitatory transmission by direct current stimulation in isolated rat hippocampus. J. Neurophysiol. 107 (7), 1881–1889.
Lee, W.H., Deng, Z.D., et al., 2011. Influence of white matter conductivity anisotropy on electric field strength induced by electroconvulsive therapy. Conf. Proc. IEEE Eng. Med. Biol. Soc. 2011, 5473–5476.
Lee, W.H., Deng, Z.D., Kim, T.S., Laine, A.F., Lisanby, S.H., Peterchev, A.V., 2012. Regional electric field induced by electroconvulsive therapy in a realistic finite element head model: influence of white matter anisotropic conductivity. Neuroimage 59 (3), 2110–2123 (Feb 1, Epub 2011 Oct 18).
Miranda, P.C., Lomarev, M., et al., 2006. Modeling the current distribution during transcranial direct current stimulation. Clin. Neurophysiol. 117 (7), 1623–1629.
Maeoka, H., Matsu, A., Hiyamizu, M., Morioka, S., Ando, H., 2012. Influence of transcranial direct current stimulation of the dorsolateral prefrontal cortex on pain related emotions: a study using electroencephalographic power spectrum analysis. Neurosci. Lett. 512 (1), 12–16.
Nitsche, M.A., Paulus, W., 2000. Excitability changes induced in the human motor cortex by weak transcranial direct current stimulation. J. Physiol. 527 (Pt. 3), 633–639.
Parazzini, M., Fiocchi, S., et al., 2012. Electric field and current density distribution in an anatomical head model during transcranial direct current stimulation for tinnitus treatment. Bioelectromagnetics 33 (6), 476–487.
Paulus, W., 2012. Transcranial electrical stimulation (tES–tDCS; tRNS, tACS) methods. Neuropsychol. Rehabil. 21 (5), 602–617.
Radman, T., Ramos, R.L., et al., 2009. Role of cortical cell type and morphology in subthreshold and suprathreshold uniform electric field stimulation in vitro. Brain Stimul. 2 (4), 215–228 (228 e211–213).
Reato, D., Rahman, A., et al., 2010. Low-intensity electrical stimulation affects network dynamics by modulating population rate and spike timing. J. Neurosci. 30 (45), 15067–15079.
Rose, K.M., Taylor, A.G., et al., 2009. Effects of cranial electrical stimulation on sleep disturbances, depressive symptoms, and caregiving appraisal in spousal caregivers of persons with Alzheimer's disease. Appl. Nurs. Res. 22 (2), 119–125.
Rose, K.M., Taylor, A.G., et al., 2008. Cranial electrical stimulation: potential use in reducing sleep and mood disturbances in persons with dementia and their family caregivers. Fam. Community Health 31 (3), 240–246.
Scherder, E.J.A., van Tol, M.J., et al., 2006. High-frequency cranial electrostimulation (CES) in patients with probable Alzheimer's disease. Am. J. Phys. Med. Rehabil. Neurophysiol. 85 (7), 614–618.
Schroeder, M.J., Barr, R.E., 2001. Quantitative analysis of the electroencephalogram during cranial electrotherapy stimulation. Clin. Neurophysiol. 112 (11), 2075–2083.
Shealy, Y.F., 1989. Synthesis and evaluation of some new retinoids for cancer chemoprevention. Prev. Med. 18 (5), 624–645.
Southworth, S., 1999. A study of the effects of cranial electrical stimulation on attention and concentration. Integr. Physiol. Behav. Sci. 34 (1), 43–53.
Suh, H.S., Lee, W.H., Cho, Y.S., Kim, J.H., Kim, T.S., 2010. Reduced spatial focality of electrical field in tDCS with ring electrodes due to tissue anisotropy. Conf. Proc. IEEE Eng. Med. Biol. Soc. 2010, 2053–2056.
Wagner, T., Fregni, F., et al., 2006. Transcranial magnetic stimulation and stroke: a computer-based human model study. Neuroimage 30 (3), 857–870.
Wagner, T., Fregni, F., et al., 2007. Transcranial direct current stimulation: a computer-based human model study. Neuroimage 35 (3), 1113–1124.
Zaghi, S., Acar, M., et al., 2010. Noninvasive brain stimulation with low-intensity electrical currents: putative mechanisms of action for direct and alternating current stimulation. Neuroscientist 16 (3), 285–307.

References for tables

Limoge, A., Robert, C., Stanley, T.H., 1999. Transcutaneous cranial electrical stimulation (TCES): A review 1998 Neuroscience and Biobehavioral Reviews 23, 529–538.
Brown, C.C., 1975. Electroanesthesia and electrosleep. Am. Psychol. 30, 402–410.
Bystritsky, A., Kerwin, L., Feusner, J., 2008. A pilot study of cranial electrotherapy stimulation for generalized anxiety disorder. J. Clin. Psychiatry. 69 (3), 412–417.
von Richthofen, Carmen L., Mellora, Clive S., 1979. Cerebral electrotherapy: methodological problems in assessing its therapeutic effectiveness. Psychol. Bull. 86, 1264–1271.
Dimitrov, D. Tz, Ralev, N.D., 2009. Signals and Systems for Electrosleep. Electron. Electric. Eng. 5 (93), 95–98.
Liss Body Stimulator, Bipolar Model No. SBL-502-B Manual.
Liss Body Stimulator, Monopolar ModelNo.SBL-501-M Manual.